Computational Modeling and Verification of Signaling Pathways in Cancer

Haijun Gong[1] Paolo Zuliani[1] Anvesh Komuravelli[1] James R. Faeder[2] Edmund M. Clarke[1]
[1]Computer Science Department, Carnegie Mellon University, Pittsburgh, PA 15213, USA
{haijung,pzuliani,anvesh,emc}@cs.cmu.edu
[2]Department of Computational Biology, University of Pittsburgh, Pittsburgh, PA 15260, USA
faeder@pitt.edu

Abstract

We propose and analyze a rule-based model of the HMGB1 signaling pathway. The protein HMGB1 can activate a number of regulatory networks – the p53, NFκB, Ras and Rb pathways – that control many physiological processes of the cell. HMGB1 has been recently shown to be implicated in cancer, inflammation and other diseases. In this paper, we focus on the NFκB pathway and construct a crosstalk model of the HMGB1-p53-NFκB-Ras-Rb network to investigate how these couplings influence proliferation and apoptosis (programmed cell death) of cancer cells. We first built a single-cell model of the HMGB1 network using the rule-based BioNetGen language. Then, we analyzed and verified qualitative properties of the model by means of simulation and statistical model checking. For model simulation, we used both ordinary differential equations and Gillespie's stochastic simulation algorithm. Statistical model checking enabled us to verify our model with respect to behavioral properties expressed in temporal logic. Our analysis showed that HMGB1-activated receptors can generate sustained oscillations of irregular amplitude for the NFκB, IκB, A20 and p53 proteins. Also, knockout of A20 can destroy the IκB-NFκB negative feedback loop, leading to the development of severe inflammation or cancer. Our model also predicted that the knockout or overexpression of the IκB kinase can influence the cancer cell's fate – apoptosis or survival – through the crosstalk of different pathways. Finally, our work shows that computational modeling and statistical model checking can be effectively combined in the study of biological signaling pathways.

1 Introduction

Computational modeling is increasingly used to gain insights into the behavior of complex biological systems, such as signaling pathways. Moreover, powerful verification methods (*e.g.*, model checking [8]) from the field of hardware verification have been recently applied to the analysis of biological system models. In this paper we build a single-cell model of the HMGB1 pathway using the rule-based BioNetGen language [21], and use statistical model checking to formally verify interesting properties of our model. We argue that computational modeling and statistical model checking can be combined into an effective tool for analyzing the emergent behavior of complex signaling pathways. In particular, the use of statistical model checking enables us to tackle large systems in a scalable way.

The High-Mobility Group Box-1 (HMGB1) protein is released from necrotic cells or secreted by activated macrophages engulfing apoptotic cells [12]. Recent studies have shown that HMGB1 and its receptors, including the Receptor for Advanced Glycation End products (RAGEs) and Toll-Like Receptors (TLRs), are implicated in cancer, inflammation and other diseases [10, 41]. Elevated expression of HMGB1 occurs in various types of tumors, including colon, pancreatic, and breast cancer [12, 33, 44]. HMGB1 can activate a number of regulatory networks – the PI3K/AKT, NFκB, and Ras pathways – which control many physiological processes including cell cycle arrest, apoptosis and proliferation. The cell cycle is strictly regulated and controlled by a number of signaling pathways that ensure cell proliferation occurs only when it is required by the organism as a whole [19]. Overexpression of HMGB1 can continuously activate cell-growth signaling pathways even if there are protein mutations or DNA damage, possibly leading to the occurrence of cancer in the future. Recent *in vitro* studies with pancreatic

cancer cells [26] have shown that the targeted knockout or inhibition of HMGB1 and its receptor RAGE can increase apoptosis and suppress cancer cell growth. This phenomenon has also been observed with lung cancer and other types of cancer cells [4, 12].

Model Checking [7, 8] is one of the most widely used techniques for the automated verification and analysis of hardware and software systems. System models are usually expressed as state-transition diagrams and a temporal logic is used to describe the desired properties (specifications) of system executions. A typical property stated in temporal logic is $\mathbf{G}(grant\_req \rightarrow \mathbf{F}\, ack)$, meaning that, it is always (**G** = globally) true that a grant request eventually (**F** = future) triggers an acknowledgment. One important aspect of Model Checking is that it can be performed algorithmically – user intervention is limited to providing a system model and a property to check. Because biological systems are often probabilistic in nature, we make use of *statistical* model checking, a technique tailored to the verification of stochastic systems (see Section 2).

In [18], we proposed the first model of HMGB1 signal transduction, based on known signaling pathway studies [6, 38, 47]. The model was used to investigate the importance of HMGB1 in tumorigenesis. In this work, we propose a single-cell model of the HMGB1 signaling pathway, which includes the NFκB pathway and a crosstalk model of the HMGB1-p53-NFκB-Ras-Rb network. The model is described by means of the rule-based BioNetGen language [21]. We analyze and verify qualitative properties of the model using simulation and statistical model checking. For model simulation, we use both ordinary differential equations (ODEs) and Gillespie's stochastic simulation algorithm [15]. Statistical model checking enables us to verify our model with respect to behavioral properties expressed in temporal logic.

Our baseline simulations show that HMGB1-activated receptors can generate sustained oscillations of irregular amplitude for the NFκB, IκB, IKK and A20 proteins. However, mutation or knockout of the A20 protein can destroy the IκB-NFκB negative feedback loop, leading to the development of severe inflammation or cancer. Further analysis shows that overexpression of HMGB1 can up-regulate the oncoproteins NFκB and Cyclin E (which regulate cell proliferation), but down-regulate the tumor-suppressor protein p53 (which regulates cell apoptosis). Also, overexpression of NFκB can increase the expression level of both Cyclin E and p53. Our model also predicts that the knockout or overexpression of the IκB kinase (IKK) can influence the cancer cell's fate – apoptosis or survival – through the crosstalk of different pathways. To the best of the authors' knowledge, this work is the first attempt to integrate the NFκB, p53, Ras, and Rb signaling pathways activated by HMGB1 in one rule-based model.

2 Statistical Model Checking

In the past few years, there has been growing interest in the formal verification of stochastic systems, and biological systems in particular [25, 28, 39], by means of model checking techniques. The verification problem is to decide whether a stochastic model satisfies a temporal logic property with a *probability* greater than or equal to a certain threshold. To express properties, we use a temporal logic in which the temporal operators are equipped with *bounds*. For example, the property "p53 will always stay below 30 in the next 80 time units" is written as $\mathbf{G}^{80}(p53 < 30)$. We ask whether our stochastic system M satisfies that formula with a probability greater than or equal to a fixed threshold (say 0.99), and we write $M \models Pr_{\geqslant 0.99}[\mathbf{G}^{80}(p53 < 30)]$. Such questions can be answered by *Statistical Model Checking* [50], the technique we use for verifying BioNetGen models simulated by Gillespie's algorithm.

Statistical model checking treats the verification problem as a statistical inference problem and solves it by randomized sampling of traces (simulations) from the model. In particular, the inference problem can be solved by means of hypothesis testing or estimation. The former amounts to deciding between two hypotheses – $M \models Pr_{\geqslant \theta}[\phi]$ versus $M \models Pr_{<\theta}[\phi]$, where θ is a given probability threshold and ϕ is a

temporal logic property. The latter, instead, approximates probabilistically (that is, it computes with high probability an *estimate* close to) the true probability p that ϕ holds, and then compares that estimate with θ. In both approaches, sampled traces are model checked individually to determine whether property ϕ holds, and the number of satisfying traces is used by the hypothesis testing (or estimation) procedure to decide between $p \geqslant \theta$ and $p < \theta$. (In the case of estimation, one also has an estimate that is close to p with high probability.) Note that statistical model checking cannot guarantee a correct answer to the verification problem. However, the probability of giving a wrong answer can be arbitrarily bounded by the user.

In the next section we describe the temporal logic used in this work, Bounded Linear Temporal Logic (BLTL) [25, 51].

2.1 Bounded Linear Temporal Logic

Let SV be a finite set of real-valued variables. An atomic proposition AP is a boolean predicate of the form $e_1 \sim e_2$, where e_1 and e_2 are arithmethic expressions over variables in SV, and $\sim$ is either $\geq$, $\leq$, or $=$. A BLTL property is built over atomic propositions using boolean connectives and bounded temporal operators. The syntax of the logic is the following:

$$\phi ::= AP \mid \phi_1 \vee \phi_2 \mid \phi_1 \wedge \phi_2 \mid \neg\phi_1 \mid \phi_1 \mathbf{U}^t \phi_2.$$

The bounded until operator $\phi_1 \mathbf{U}^t \phi_2$ requires that, *within* time t, ϕ_2 will be true and ϕ_1 will hold until then. Bounded versions of the **F** and **G** operators can be easily defined: $\mathbf{F}^t \phi = true\ \mathbf{U}^t \phi$ requires ϕ to hold true within time t; $\mathbf{G}^t \phi = \neg \mathbf{F}^t \neg \phi$ requires ϕ to hold true up to time t.

The semantics of BLTL is defined with respect to *traces* (or executions) of a system. In our case, a trace will be the output of a BioNetGen model simulated by Gillespie's algorithm. Formally, a trace is a sequence of time-stamped state transitions of the form $\sigma = (s_0, t_0), (s_1, t_1), ...$, where (s_i, t_i) denotes that the system moved to state s_{i+1} after having sojourned for t_i time units in state s_i. The fact that a trace σ satisfies the BLTL property ϕ is written $\sigma \models \phi$. We denote the trace suffix starting at step k by σ^k. We have the following semantics of BLTL:

- $\sigma^k \models AP$ if and only if AP holds true in state s_k;
- $\sigma^k \models \phi_1 \vee \phi_2$ if and only if $\sigma^k \models \phi_1$ or $\sigma^k \models \phi_2$;
- $\sigma^k \models \phi_1 \wedge \phi_2$ if and only if $\sigma^k \models \phi_1$ and $\sigma^k \models \phi_2$;
- $\sigma^k \models \neg\phi_1$ if and only if $\sigma^k \models \phi_1$ does not hold;
- $\sigma^k \models \phi_1 \mathbf{U}^t \phi_2$ if and only if there exists $i \in N$ such that, (a)$\sum_{0 \leq l < i} t_{k+l} \leq t$, (b) $\sigma^{k+i} \models \phi_2$ and (c) for each $0 \leq j < i$, $\sigma^{k+j} \models \phi_1$.

Note that the semantics of BLTL is defined over *infinite* traces, while of course any simulation trace must be finite in length. It can be shown that traces of an appropriate (finite) length are sufficient to decide BLTL properties. The interested reader can find details elsewhere [51].

2.2 Bayesian Statistical Model Checking

We recently introduced sequential Bayesian hypothesis testing and estimation techniques and applied them to the verification of signaling pathways and other stochastic systems [25, 51]. Sequential sampling means that the number of sampled traces is not fixed a priori, but it is instead determined at "run-time," depending on the evidence gathered by the samples seen so far. This often leads to a significantly smaller number of sampled traces. Both approaches are based on Bayes' theorem, which enables us to use prior information about the model being verified, where available. We now briefly describe both techniques.

Bayesian Hypothesis Testing. The hypothesis test is based on the Bayes Factor, which is the likelihood ratio of the sampled data with respect to the two hypotheses. For statistical model checking, the hypotheses being tested are $H_0 : p \geqslant \theta$ and $H_1 : p < \theta$, where p is the (unknown) probability that our model satisfies a given property, and θ is a probability threshold. Formally, the Bayes Factor of data d and hypotheses H_0 and H_1 is $B = \frac{Pr(d|H_0)}{Pr(d|H_1)}$. Therefore, B can be interpreted as a measure of evidence (given by the data d) in favor of H_0. Now, fix an evidence threshold $T > 1$. Our algorithm iteratively draws independent and identically distributed (iid) sample traces $\sigma_1, \sigma_2, \ldots$, and checks whether they satisfy ϕ. After each trace, the algorithm computes the Bayes Factor B to check if it has obtained conclusive evidence. The algorithm accepts H_0 if $B > T$, and rejects H_0 (accepting H_1) if $B < \frac{1}{T}$. Otherwise (if $\frac{1}{T} \leqslant B \leqslant T$), it continues drawing iid samples. It can be shown that when the algorithm terminates, the probability of a wrong answer is bounded above by $\frac{1}{T}$. The algorithm is shown below in Algorithm 1 – full details can be found elsewhere [51].

Algorithm 1 Statistical Model Checking by Bayesian Hypothesis Testing

Require: BLTL Property ϕ, Probability threshold $\theta \in (0,1)$, Threshold $T > 1$, Prior density g for unknown parameter p

```
n := 0                                   {number of traces drawn so far}
x := 0                                   {number of traces satisfying φ so far}
loop
  σ := draw a sample trace of the system (iid)
  n := n + 1
  if σ ⊨ φ then
    x := x + 1
  end if
  B := BayesFactor(n, x)                 {compute the Bayes Factor}
  if (B > T) then
    return H0 accepted
  else if (B < 1/T) then
    return H1 accepted
  end if
end loop
```

Bayesian Interval Estimation. Recall that in estimation, we are interested in computing a value (an estimate) which is close to p with high probability, the true probability that the model satisfies the property. The estimate is usually in the form of a confidence interval – an interval in $[0,1]$ which contains p with high probability. Our estimation method follows directly from Bayes' theorem. Given a prior distribution over p and sampled data, Bayes' theorem enables us to obtain the *posterior* distribution of p (*i.e.*, the distribution of p given the data sampled and the prior). This means that we can estimate p with the mean of the posterior distribution. Furthermore, by integrating the posterior over a suitably chosen interval, we can compute a Bayes interval estimate with any given confidence coefficient. Fix a confidence $c \in (\frac{1}{2}, 1)$ and a half-width $\delta \in (0, \frac{1}{2})$. Our algorithm iteratively draws iid traces, checks whether they satisfy ϕ, and builds an interval of total width 2δ, centered on the posterior mean. If the integral of the posterior over this interval is greater than c, the algorithm stops; otherwise, it continues sampling. The algorithm is given in Algorithm 2. Again, full details are given in [51].

Algorithm 2 Statistical Model Checking by Bayesian Interval Estimates

Require: BLTL Property ϕ, half-interval size $\delta \in (0, \frac{1}{2})$, interval coefficient $c \in (\frac{1}{2}, 1)$, Prior Beta distribution with parameters α, β

```
n := 0                                  {number of traces drawn so far}
x := 0                                  {number of traces satisfying φ so far}
repeat
  σ := draw a sample trace of the system (iid)
  n := n + 1
  if σ ⊨ φ then
    x := x + 1
  end if
  p̂ := (x + α)/(n + α + β)              {compute posterior mean}
  (t0, t1) := (p̂ − δ, p̂ + δ)            {compute interval estimate}
  if t1 > 1 then
    (t0, t1) := (1 − 2·δ, 1)
  else if t0 < 0 then
    (t0, t1) := (0, 2·δ)
  end if
  {compute posterior probability of p ∈ (t0, t1)}
  γ := PosteriorProb(t0, t1)
until (γ ⩾ c)
return (t0, t1), p̂
```

3 Crosstalk Model of HMGB1

Apoptosis and cell proliferation are two important processes in cancer and are respectively regulated by two proteins – p53 and Cyclin E – acting in two different signaling pathways. The protein p53 is a tumor suppressor whose activation can lead to cell cycle arrest, DNA repair or apoptosis. Cyclin E is a cell cycle regulatory protein that regulates the G1-S phase transition during cell proliferation. The behavior of these two signaling pathways can be influenced by crosstalk or coupling with other pathways and proteins.

3.1 Motivations

Experimental studies have shown that HMGB1 can activate three fundamental downstream signaling pathways: the PI3K/AKT, RAS-ERK and NFκB pathways. These in turn lead to the activation of two other signaling pathways: the p53-MDM2 and Rb-E2F pathways, which regulate apoptosis and cell proliferation, respectively. In [18], we proposed the first computational model for HMGB1 signal transduction (also called the NFκB-knockout model). The model included the p53-MDM2, Ras-ERK, and Rb-E2F pathways and was able to explain qualitatively some existing experimental phenomena in tumorigenesis. One of our goals in this work is to integrate the NFκB signaling pathway into our previous NFκB-knockout model in order to explain recent results linking overexpression of HMGB1 with a decrease of apoptosis (and increased cancer cell survival).

The NFκB protein is involved in a variety of cellular processes, including inflammation, cell proliferation and apoptosis. Studies have shown that NFκB is also a transcription factor for the pro-apoptotic gene p53 [48], for anti-apoptotic genes, including Bcl-XL [23] and for the cell-cycle regulatory proteins

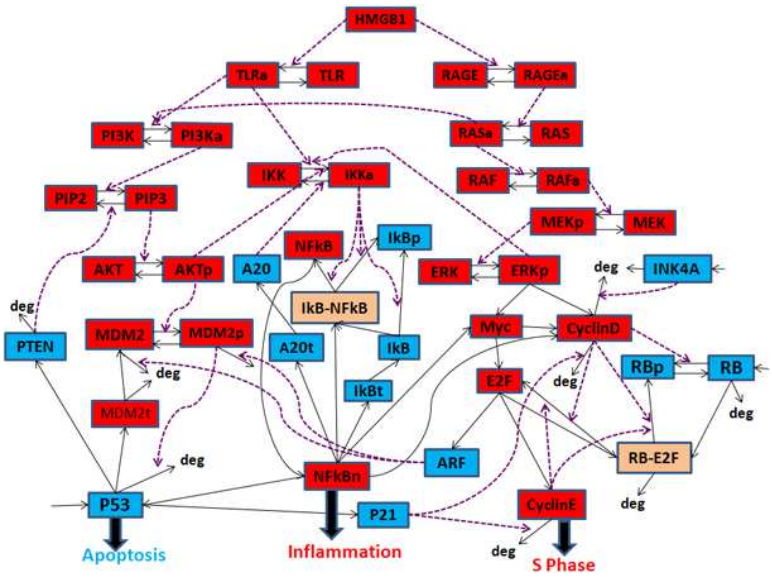

Figure 1: Schematic view of HMGB1 signal transduction. Blue nodes represent tumor suppressor proteins; red nodes represent oncoproteins/lipids; brown nodes represent protein complexes. Solid lines with arrows denote protein transcription, degradation or changes of molecular species; dashed lines with arrows denote activation processes.

Myc and Cyclin D [20]. We aim to understand how the NFκB pathway influences the HMGB1 signal transduction pathway.

Recent experiments with mammalian cells [22, 36] have found oscillations of NFκB, activated by tumor necrosis factor (TNF), with a time period in the order of hours. Several mathematical models based on ODEs were constructed to study the NFκB system [22, 27, 32]. Since biological systems are intrinsically stochastic, our goal is to study the oscillations of NFκB's expression level in the nucleus and compare the stochastic simulation results with the ODEs results.

Finally, the NFκB pathway is regulated by many proteins including A20, IKK and NFκB. The overexpression or mutation of IKK and NFκB [5, 11] occur frequently in many cancer types. We aim to investigate how these proteins' mutation or overexpression changes the cell's fate – apoptosis or survival.

3.2 Model Formulation

In Fig. 1, we illustrate the crosstalk model of the HMGB1 signaling pathway. It includes 44 molecular species (nodes), 82 chemical reactions, and four coupling signaling pathways: the RAS-ERK, Rb-E2F, IKK-NFκB and p53-MDM2 pathways. We now briefly describe these signaling pathways and their interplay with the NFκB network. We denote activation (or promotion) by $\rightarrow$ and inhibition (or repression) by $\dashv$.

The p53-MDM2 pathway is regulated by a negative feedback loop: TLR $\rightarrow$ PI3K $\rightarrow$ PIP3 $\rightarrow$ AKT $\rightarrow$ MDM2 $\dashv$ p53 $\rightarrow$ MDM2, and a positive feedback loop: p53 $\rightarrow$ PTEN $\dashv$ PIP3 $\rightarrow$ AKT $\rightarrow$ MDM2 $\dashv$ p53 $\rightarrow$ Apoptosis [29]. The protein PI3K is activated by the toll-like receptors (TLR2/4) [45] and can phosphorylate the lipid PIP2 to PIP3, leading to the phosphorylation of AKT. The oncoprotein MDM2 can only reside in the cytoplasm before it is phosphorylated by AKT. The phosphorylated MDM2 can enter the nucleus to bind with p53, inhibit p53's transcriptional activity and target it for degradation. The protein p53 can also induce the transcription of another tumor suppressor protein, PTEN, which can

hydrolyze PIP3 to PIP2 and inhibit the phosphorylation of MDM2.

The RAS-ERK pathway is RAGE $\rightarrow$ RAS $\rightarrow$ RAF $\rightarrow$ MEK $\rightarrow$ ERK. Upon activation by HMGB1, RAGE will activate the RAS proteins, leading to a cascade of events including the activation and phosphorylation of the RAF, MEK and ERK1/2 proteins. The mutated K-RAS protein, a member of the RAS protein family, can continuously activate the downstream cell cycle signaling pathways. The activated ERK can enter the nucleus and phosphorylate transcription factors which induce the expression of cell cycle regulatory proteins, such as Cyclin D and Myc (see Fig. 1).

The Rb-E2F pathway is Cyclin D $\dashv$ Rb $\dashv$ E2F $\rightarrow$ Cyclin E $\dashv$ Rb. This pathway plays an important role in the regulation of the G1-S phase transition in the cell cycle. In particular, E2F is a transcription factor that regulates the expression of a set of cell-cycle regulatory genes [49]. In resting cells, E2F's transcriptional activity is repressed by the unphosphorylated Rb, a tumor suppressor protein, through the formation of an Rb-E2F complex. The oncoproteins Cyclin D and Myc can phosphorylate the Rb protein, which can then activate E2F. In turn, E2F activates the transcription of Cyclin E and Cyclin-dependent protein kinase 2 (CDK2), which promotes cell-cycle progression from G1 to S phase. Cyclin E can also phosphorylate and inhibit Rb, leading to a forward positive feedback loop [42, 37]. The protein INK4A is another important tumor suppressor that can repress the activity of Cyclin D-CDK4/6 and inhibit E2F's transcriptional activity and cell cycle progression. It is known that INK4A is mutated in over 90% of pancreatic cancers [3].

The NFκB pathway is regulated by two negative feedback loops: TLR $\rightarrow$ IKK $\dashv$ IκB $\dashv$ NFκB $\rightarrow$ IκB $\dashv$ NFκB, and NFκB $\rightarrow$ A20 $\dashv$ IKK $\dashv$ IκB $\dashv$ NFκB. In the resting wild-type cells, IκB resides only in the cytoplasm where it is bound to NFκB. Upon being activated by HMGB1, TLR2/4 can signal via MyD88, IRAKs and TRAF to activate and transform IκB kinase (IKK) into its active form IKKa, leading to the phosphorylation, ubiquitination and degradation of IκB. The free NFκB rapidly enters the nucleus to bind to specific κB sites in the A20 and IκB promoters, activating their expression. The newly synthesized IκB enters the nucleus to bind to NFκB and takes it out into the cytoplasm to inhibit its transcriptional activity. Moreover, the newly synthesized A20 can also inhibit IKK's activity, leading to inhibition of NFκB.

Besides the main signal transduction, the interplay between these four signaling pathways can influence the cell's fate. As shown in Fig. 1, RAS can activate the PI3K-AKT signaling pathway; ERK and AKT can activate IKK in the NFκB pathway. The tumor suppressor protein ARF, activated by the overexpressed oncoprotein E2F, can bind to MDM2 to promote its degradation and stabilize p53's expression level, leading to apoptosis. Moreover, it has been demonstrated [46] that the p53-dependent tumor suppressor proteins p21 and FBXW7 can restrain the activity of Cyclin D-CDK4/6 and Cyclin E-CDK2 (only p21 is shown in Fig. 1 to represent both p21 and FBXW7's contribution). Mutations of RAS, ARF, P21 and FBXW7 have been found in many cancers [3, 9]. NFκB is a transcription factor for p53, Myc and Cyclin D, regulating cell proliferation and apoptosis. The overexpression of NFκB occurs in approximately 80% of lung cancer cases [43], and it is also common in pancreatic cancer [5]. Our model and simulation will investigate how these mutations and overexpressions affect the cell's fate.

3.3 Simulation Models

Similar to the model in our previous work [18], in this model (see Fig. 1), all substrates are expressed in terms of the number of molecules. A protein with the subscript "*a*", "*p*" or "*t*" corresponds respectively to active form, phosphorylated form or mRNA transcript of the protein. For example:

- AKT (AKT_p) - unphosphorylated (phosphorylated) AKT.
- RAS (RAS_a) - inactive (active) RAS.

- IκB$_t$ - mRNA transcript of IκB.

We sometimes use CD to stand for the Cyclin D-CDK4/6 complex, CE for the Cyclin E-CDK2 complex, RE for the Rb-E2F complex, and IκNF for the (IκB|NFκB) or (IκB-NFκB) dimer. We also assume that the total number of active and inactive forms of the RAGE, TLR, PI3K, IKK, PIP, AKT, RAS, RAF, MEK, ERK and NFκB molecules is constant [18]. For example, AKT + AKT$_p$ = AKT$_{tot}$, PIP2 + PIP3 = PIP$_{tot}$ and NFκB + NFκB$_n$ + (IκB|NFκB) = NFκB$_{tot}$.

We have formulated a reaction model corresponding to the reactions illustrated in Fig. 1 in the form of rules specified in the BioNetGen language [21]. We use Hill functions to describe the rate laws governing the transcription of some proteins, including PTEN, MDM2, CyclinD (CD), Myc, E2F, CyclinE (CE), A20 and IκB, and use mass action rules for other reactions. We use both ODEs and Gillespie's stochastic simulation algorithm (SSA) [15] to simulate the same model with BioNetGen. Stochastic simulation is important because when the number of molecules involved in the reactions is small, stochasticity and discretization effects become more prominent [17, 16, 31]. The ODEs for the NFκB-knockout HMGB1 model have been provided in our previous work [18]. The ODEs for the HMGB1-p53-Ras-NFκB-Rb crosstalk model are listed in the online supplementary materials [2]. We now give an example to illustrate how to convert an ODE into BioNetGen rules. The ODE for the phosphorylated $AKT - AKT_p$ is

$$\frac{d}{dt}AKT_p(t) = k_4 PIP3(t)AKT(t) - d_4 AKT_p(t),$$

where the first term describes the phosphorylation of AKT, activated by PIP3. The second term describes AKT$_p$ dephosphorylation. In BioNetGen, the molecule type $AKT(a \sim U \sim p)$ has a component named a with state label U (unphosphorylated) and p (phosphorylated). The BioNetGen rules for the ODE above are:

$$AKT(a \sim U) + PIP3 \rightarrow AKT(a \sim p) + PIP3 \;\; k4;$$

$$AKT(a \sim p) \rightarrow AKT(a \sim U) \;\; d4;$$

where k_4 and d_4 are the constants for AKT phosphorylation and dephosphorylation rates, respectively. The interested reader can refer to the BioNetGen tutorial [13] for details. The BioNetGen code of our model is available online [1]. The model contains a large number of undetermined parameters which are difficult to estimate from available experimental data or from the literature. We emphasize that in this work, the values for several undetermined parameters listed in [2] have been chosen in order to produce a qualitative agreement with previous experiments.

4 Simulation Results

To validate the properties of the HMGB1 signal transduction model, we have conducted a series of deterministic and stochastic simulations and compared our results with known experimental facts. In our model, the p53-MDM2 and NFκB signaling pathways are regulated by two feedback loops. Recent experimental results have shown that p53's and MDM2$_p$'s expression levels undergo oscillations in response to stress signals. For example, oscillations lasted more than 72 hours after γ irradiation in Geva-Zatorsky et al.'s experiment [14]. Also, Hoffmann's experiment found oscillations of NFκB in response to TNF stimulation, with four equally spaced peaks over the course of the 6-hour experiment [22].

We first conducted baseline simulations for several important proteins involved in the HMGB1 signaling pathway. In our simulations, we set the initial value for the number of HMGB1 molecules to be 10^2; the nonzero initial values for other proteins are listed in Table 1. The input parameters and reaction descriptions are listed in the online supplementary materials [2].

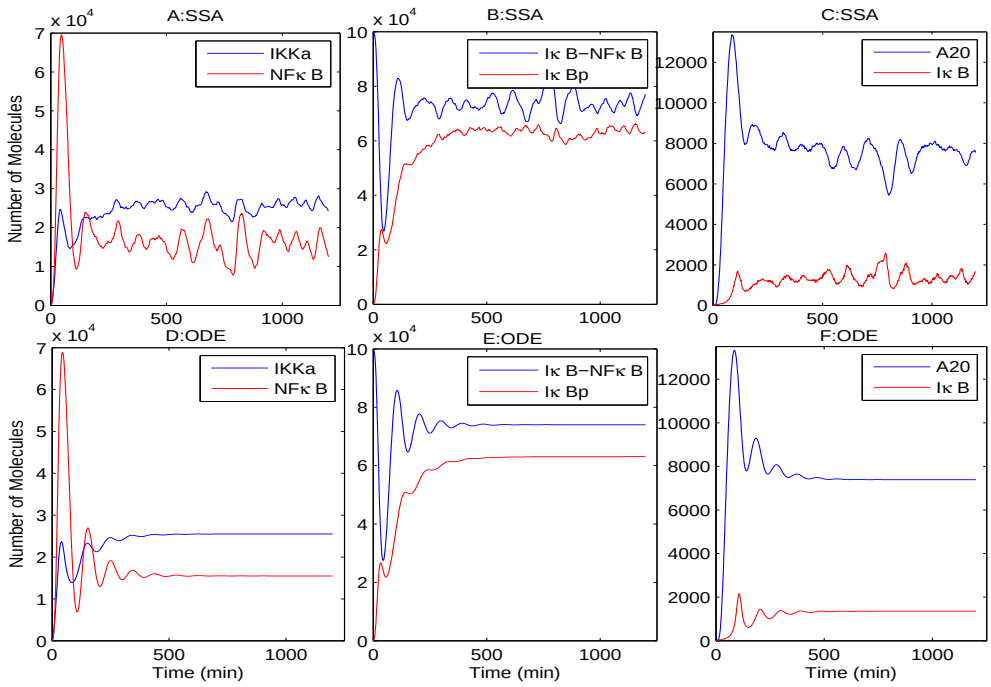

Figure 2: Number of IKKa, NFκB (A,D), IκB$_p$, IκB-NFκB complex (B,E), IκB and A20 (C,F) molecules versus time for baseline simulations with SSA(A-C) and ODE(D-F) models.

Table 1: Initial values for the proteins in the crosstalk model of HMGB1

Proteins	TLR	PI3K	PIP2	AKT	MDM2	MDM2$_p$	p53	IκB-NFκB
# of Mol.	10^3	10^5	10^5	10^5	10^4	2×10^4	2×10^4	10^5
Proteins	RAGE	RAS	RAF	MEK	ERK	RE	IKK	
# of Mol.	10^3	10^4	10^4	10^4	10^4	10^4	10^5	

In Fig. 2, we give the dynamic of the NFκB, IKK, IκB-NFκB complex, IκB, and A20 proteins using both stochastic simulation and ODEs. In Fig. 2 (A,D), we see that IKK, upon being stimulated by HMGB1, is activated immediately by the TLR, AKT and ERK proteins. This leads to the phosphorylation of IκB isoform (Fig. 2 B,E), which in turn allows NFκB to translocate into the nucleus. There, NFκB binds to the DNA and induces the transcription of the IκB and A20 inhibitor genes (Fig. 2 C,F). The synthesized IκB can enter the nucleus and recapture NFκB back into the cytoplasm to form the IκB-NFκB complex. However, IκB is continuously phosphorylated and degraded, resulting in the continued translocation of NFκB. The stochastic simulation of HMGB1-induced NFκB oscillation depicted in Fig. 2A fits very well with Nelson's experimental results [36] – the oscillation of NFκB continued for more than 20 hours after continuous TNFα stimulation, damping slowly with a period of 60-100 minutes. However, the ODEs simulation results in Fig. 2D show no NFκB oscillation after 500 minutes, when the cell reaches the resting state. The phosphorylation of IκB leads to the decrease of the IκB-NFκB complex in Fig. 2(B,E). The A20 protein can inactivate IKK to stabilize the IκB-NFκB complex. The stochastic simulation shows continuous oscillation (Fig. 2C) in 20 hours, but no oscillation is present in the ODE simulation (Fig. 2F) after 400 minutes. This discrepancy shows that in modeling signal transduction, it

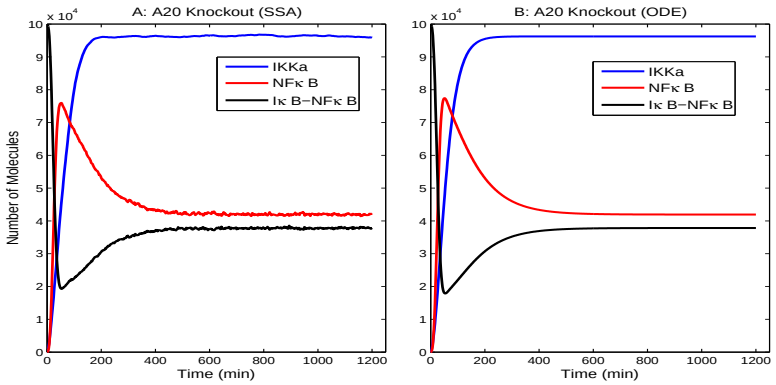

Figure 3: Number of IKKa, NFκB, IκB-NFκB molecules versus time for baseline simulations in the A20-knockout model.

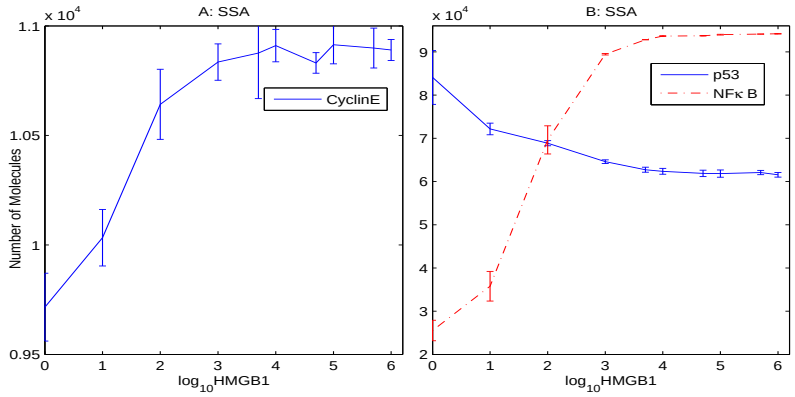

Figure 4: Overexpression of HMGB1 leads to the increase of DNA replication proteins Cyclin E and Nuclear Factor NFκB and the decrease of p53 with the SSA model.

is important to capture accurately both the discretization and stochasticity of chemical reactions. Similar stochastic oscillations of p53 and MDM2 proteins are shown in the online supplementary materials [2].

The A20 protein plays an important role in the regulation of the NFκB network. It is known that A20 knockout can result in severe inflammation and tissue damage in multiple organs [24]. As Fig. 3 shows, when A20 is knocked out, over 90% of IKK is activated, which can then phosphorylate and ubiquitinate IκB. This leads to the disassembly of the IκB-NFκB dimer and liberation of NFκB, which rapidly translocates into the nucleus. The A20-knockout results in Fig. 3 demonstrate that the oscillation of NFκB dampens very quickly, with a small period compared to Fig. 2A. This phenomenon is consistent with Mengel *et al.*'s discovery that A20 can not only dampen the oscillations, but also control the oscillation period of NFκB [35]. So, the loss of A20 can destroy the IκB-NFκB negative feedback loop. The precise role of the A20 negative feedback remains to be elucidated in future experiments.

A number of studies have found that overexpression of HMGB1 and its receptors is associated with cancer [12, 33]. Our recent NFκB-knockout HMGB1 model [18] qualitatively explained the experimental result that overexpression of HMGB1 decreases apoptosis and promotes DNA replication and proliferation in cancer cells. We now ask the following question: How do the expression levels of HMGB1 and other proteins influence the cell's fate when the NFκB signaling pathway is integrated?

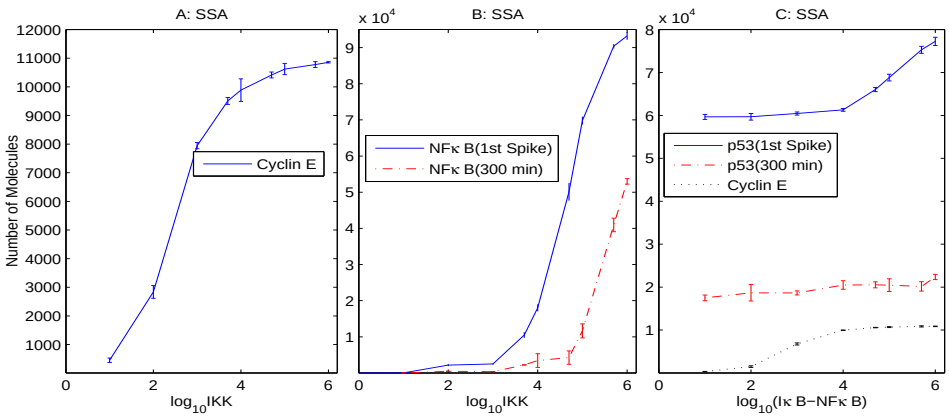

Figure 5: Overexpression of IKK lead to the increase of Cyclin E and NFκB (A-B); overexpression of NFκB increases Cyclin E and p53's concentration (C).

In Fig. 4, we varied the level of HMGB1 to determine how it affects cell behavior. We increased the number of HMGB1 molecules from 1 to 10^6, and Cyclin E's expression level at 300 minutes, and the first maximum of p53 and NFκB in phase G1 were measured using stochastic simulation. All the experiments were repeated 10 times per value to compute the mean and standard errors. In Fig. 4, we see that an increase of HMGB1's initial value can increase the number of Cyclin E and NFκB molecules, and decrease p53's expression level. With respect to our previous model [18], we see that the expression level of Cyclin E and p53 are higher, since NFκB can induce the transcription of p53, Cyclin D and Myc, which can activate the expression of Cyclin E during cell cycle progression. Therefore, the knockout of HMGB1 and its receptors can inhibit the expression of NFκB and Cyclin E, leading to cell cycle arrest or inhibition of cancer cell proliferation.

The expression of the IKK protein is elevated in many cancer cells [11]. Since IKK regulates NFκB's DNA-binding activity, we investigated how the dynamic of IKK influences the expression levels of the cell-cycle regulatory proteins Cyclin E and NFκB. We increased the number of IKK molecules and measured Cyclin E's expression level at 300 minutes. As for NFκB, we measured two values: the first maximum and the expression level at 300 minutes. In Fig. 5(A,B) we see that with the increase of IKK's expression level, Cyclin E and NFκB's concentrations increase quickly, since more active IKK can promote NFκB's DNA-binding and transcriptional activity, accelerating the progression of cell proliferation or inflammation.

It has been observed that NFκB plays a key role in the development and progression of cancer, including proliferation, migration and apoptosis [5]. Aberrant or constitutive NFκB activation has been detected in many cancers [5, 43]. Furthermore, overexpression of NFκB is very common in pancreatic cancer [5]. In our model, we set the initial value for NFκB to 0, so that NFκB is only found in the form of the transient IκB-NFκB dimer. In Fig. 5C, we increased the initial value of IκB-NFκB dimers and measured the pro-apoptotic protein p53 and cell-cycle regulatory protein Cyclin E's expression level. The results demonstrate that the overexpression of NFκB can increase Cyclin E's concentration, thereby promoting cancer cell proliferation. However, for the pro-apoptotic protein p53, the simulations show that the amplitude of p53's first maximum increases sharply when the number of NFκB-IκB dimers is over 10^4. The expression level at 300 minutes (in the steady state) is almost stable even when the number of NFκB-IκB dimers reach 10^6. This is because p53's expression level is regulated by its negative regulator MDM2 and stays at a low level in the resting state. Fig. 5 explains the experimental discovery that the overexpression of IKK and NFκB decreases apoptosis and promotes DNA replication

Table 2: Verification of Property 1 ($HMGB1 = 10^2$)

Property: $Pr_{\geqslant 0.9}[\mathbf{F}^t(NF\kappa B_n/NF\kappa B_{tot} \geqslant a)]$					
t(min)	a	# of Samples	# of Successes	Result	Time (s)
30	0.4	22	22	True	21.30
30	0.45	92	87	True	92.86
30	0.5	289	45	False	537.74
60	0.65	22	22	True	26.76

and proliferation in cancer cells [5, 11] (though NFκB could also induce the transcription of p53).

The results visualized in Fig. 4 and Fig. 5 provide some ways to inhibit tumor cell proliferation and induce tumor cell apoptosis through inhibition or deactivation of the HMGB1 and NFκB signaling pathways. This can be achieved, for example, via the inhibition of IKK and NFκB's transcription activity on Cyclin D and Myc. Recently, the targeting of IKK and IKK-related kinases has become a popular avenue for therapeutic interventions in cancer [30]. Inhibitor drugs for NFκB's upstream protein RAS [34, 40], and downstream protein CDK, have also been developed to inhibit tumor growth.

5 Verification of the HMBG1 Pathway

We applied statistical model checking to formally verify several important properties related to NFκB. We first applied the Bayesian Hypothesis Testing method to verify the properties in the stochastic HMGB1 model. We tested whether our model satisfied a given BLTL property with probability $p \geqslant 0.9$. We set the Bayesian Hypothesis Testing threshold $T = 1000$, so the probability of a wrong answer was smaller than 10^{-3}.

Property 1: It is known that NFκB in the nucleus increases quickly after IκB is phosphorylated by IKK, which is activated by HMGB1 after approximately 30-60 minutes. Let $R = \frac{NF\kappa B_n}{NF\kappa B_{tot}}$ be the fraction of NFκB molecules in the nucleus. We verified the following property

$$Pr_{\geqslant 0.9}[\mathbf{F}^t(R \geqslant a)],$$

which informally means that the fraction of NFκB molecules in the nucleus will eventually be greater than a threshold value a within t minutes. We verified this property with various values of a and t. The results are shown in Table 2.

Property 2: The IκB and A20 proteins, which are NFκB's transcription targets, inhibit the expression of NFκB, leading to the oscillation of NFκB's expression level. We verified the property

$$Pr_{\geqslant 0.9}[\mathbf{F}^t(R \geqslant 0.65 \;\&\; \mathbf{F}^t(R \leqslant 0.20 \;\&\; \mathbf{F}^t(R \geqslant 0.20 \;\&\; \mathbf{F}^t(R \leqslant 0.20))))] \;.$$

That is, the fraction of NFκB molecules in the nucleus is oscillating: R will eventually be greater than 65% within t minutes, it will then fall below 20% within another t minutes, will increase over 20% within the following t minutes, and will finally decrease to 20% within another t minutes. We verified this property with various values of t and HMGB1, and the results are shown in Table 3.

Property 3: A large proportion of PI3K, RAS and IKK molecules can be activated when the over-expressed HMGB1 binds to RAGE and TLRs. We verified the following property

$$Pr_{\geqslant 0.9}[\mathbf{F}^t\mathbf{G}^{180}(PI3K_a/PI3K_{tot} > 0.9 \;\&\; RAS_p/RAS_{tot} > 0.8 \;\&\; IKK_a/IKK_{tot} > 0.6)],$$

Table 3: Verification of Property 2

Property: $Pr_{\geqslant 0.9}[\mathbf{F}^t(R \geqslant 0.65 \;\&\; \mathbf{F}^t(R \leqslant 0.20 \;\&\; \mathbf{F}^t(R \geqslant 0.20 \;\&\; \mathbf{F}^t(R \leqslant 0.20))))]$					
HMGB1	t(min)	# of Samples	# of Successes	Result	Time (s)
10^2	45	13	1	False	76.77
10^2	60	22	22	True	111.76
10^2	75	104	98	True	728.65
10^5	30	4	0	False	5.76

Table 4: Verification of Property 3 and 4

Property 3					Property 4				
t(min)	Samples	Successes	Result	Time (s)	IKK	Samples	Successes	Result	Time (s)
90	9	0	False	21.27	10^5	22	22	True	547.52
110	38	37	True	362.19	2×10^4	9	2	False	55.86
120	22	22	True	214.38	10^2	4	0	False	16.89

which means that 90% of PI3K, 80% of RAS and 60% of IKK will be activated within t minutes, and they will always stay above these values during the next 3 hours. This property was tested with HMGB1 overexpressed (10^5) and for various values of t given in Table 4.

Property 4: The overexpression of IKK can promote the translocation of NFκB into the nucleus, induce the transcription of protein Cyclin D and Myc and lead to the overexpression of Cyclin E. We verified the property

$$Pr_{\geqslant 0.9}[\mathbf{F}^{300}\mathbf{G}^{300}(CyclinE >= 10,000)].$$

The results are presented in Table 4.

We also used the Bayesian interval estimation algorithm to perform a more accurate study of several temporal properties. In Table 5, we report the estimates for the probability that the HMGB1-NFκB model satisfies three temporal logic properties. We ran the tests with uniform prior and half-interval size $\delta = 0.01$ and coverage probability $c = 0.9$. We can see from the computation time of the tables that statistical model checking is feasible even with large reaction networks, such as the one under study.

6 Discussion

This paper is the first attempt to integrate the NFκB signaling pathway with the p53-MDM2 and Rb-E2F pathways to study HMGB1 signal transduction at the single cell level. The NFκB pathway is important

Table 5: Bayesian Estimation of Temporal Logic Properties

IKK	Property	Posterior Mean	# of Samples	Time (s)
10^5	$[\mathbf{F}^{30}(NF\kappa B_n/NF\kappa B_{tot} \geqslant 0.45)]$	0.9646	903	464
10^5	$[\mathbf{F}^{60}(NF\kappa B_n/NF\kappa B_{tot} \geqslant 0.65 \;\&\; \mathbf{F}^{60}(NF\kappa B_n/NF\kappa B_{tot} \leqslant 0.2))]$	0.9363	689	1783
10^2	$[\mathbf{F}^{300}\mathbf{G}^{300}(CyclinE >= 10,000)]$	0.0087	113	252.83

because it regulates the transcription of many pro-apoptotic and anti-apoptotic proteins. Several experiments were simulated using ODEs and Gillespie's algorithm under a range of conditions, using the BioNetGen language and simulator. We used statistical model checking to formally and automatically validate our model with respect to a selection of temporal properties. Model validation is performed efficiently and in a scalable way, thereby promising to be feasible even for larger BioNetGen models.

Our stochastic simulations show that HMGB1-activated receptors can generate sustained oscillations of irregular amplitude for several proteins including NFκB, IKK and p53. These results are qualitatively confirmed by experiments on p53 [14] and NFκB [36]. The simulations also demonstrate a dose-dependent p53, Cyclin E and NFκB response curve to an increase in HMGB1 stimulus, which is qualitatively consistent with experimental observations in cancer studies [26, 44]. In particular, overexpression of HMGB1 can promote the expression of the cell cycle regulatory proteins Cyclin E and NFκB. It can also inhibit the pro-apoptotic p53 protein, which can lead to increased cancer cell survival and decreased apoptosis. We also investigated how the mutation or knockout of the IKK, A20 and NFκB proteins influence the fate of cancer cells.

Moreover, understanding of HMGB1 at the mechanistic level is still not clear, and reaction rates for some proteins interactions in the four signaling pathways have not been measured by experiments. We have also made some simplifications and assumption in our model. For example, the NFκB protein complex is composed of RelA(p65), RelB, cRel and NFκB1(p50), but we neglected the formation of the NFκB complex in our HMGB1 model in order to make the model relatively simple.

Our current HMGB1-Ras-p53-NFκB-Rb crosstalk model compares qualitatively well with experiments, and can provide valuable information about the behavior of HMGB1 signal transduction in response to different stimuli. In the future we plan to improve further our model with the help of new experimental results. Furthermore, the use of model checking techniques will enable us identifying and validating more realistic models.

7 Acknowledgments

This work was supported by a grant from the U.S. National Science Foundation's Expeditions in Computing Program (award ID 0926181). The authors thank Michael T. Lotze (University of Pittsburgh) for calling their attention to HMGB1 and for helpful discussions on the topic. H.G. would like to thank Marco E. Bianchi (San Raffaele University) for email discussions on HMGB1. The authors would also like to thank Ilya Korsunsky and Máté L. Nagy for their comments on this paper.

References

[1] HMGB1-NFkB BioNetGen Code. `http://www.cs.cmu.edu/~haijung/research/HMGB1ANB.bngl`.

[2] Online Supplementary Materials. `http://www.cs.cmu.edu/~haijung/research/ANBSupplement.pdf`.

[3] N. Bardeesy and R. A. DePinho. Pancreatic cancer biology and genetics. *Nature Reviews Cancer*, 2(12):897–909, 2002.

[4] M. L. Brezniceanu, K. Volp, S. Bosser, C. Solbach, P. Lichter, et al. HMGB1 inhibits cell death in yeast and mammalian cells and is abundantly expressed in human breast carcinoma. *FASEB Journal*, 17:1295–1297, 2003.

[5] S. Cascinu, M. Scartozzi, et al. COX-2 and NF-kB overexpression is common in pancreatic cancer but does not predict for COX-2 inhibitors activity in combination with gemcitabine and oxaliplatin. *American Journal of Clinical Oncology*, 30(5):526–530, 2007.

[6] A. Ciliberto, B. Novak, and J. Tyson. Steady states and oscillations in the p53/Mdm2 network. *Cell Cycle*, 4(3):488–493, 2005.

[7] E. M. Clarke, E. A. Emerson, and J. Sifakis. Model checking: algorithmic verification and debugging. *Commun. ACM*, 52(11):74–84, 2009.

[8] E. M. Clarke, O. Grumberg, and D. A. Peled. *Model Checking*. MIT Press, 1999.

[9] J. Downward. Targeting RAS signalling pathways in cancer therapy. *Nature Reviews Cancer*, 3:11–22, 2003.

[10] I. E. Dumitriu, P. Baruah, B. Valentinis, et al. Release of high mobility group box 1 by dendritic cells controls T cell activation via the receptor for advanced glycation end products. *The Journal of Immunology*, 174:7506–7515, 2005.

[11] S.F. Eddy, S. Guo, et al. Inducible IkB kinase/IkB kinase expression is induced by CK2 and promotes aberrant Nuclear Factor-kB activation in breast cancer cells. *Cancer Research*, 65:11375–11383, 2005.

[12] J. E. Ellerman, C. K. Brown, M. de Vera, H. J. Zeh, T. Billiar, et al. Masquerader: high mobility group box-1 and cancer. *Clinical Cancer Research*, 13:2836–2848, 2007.

[13] J.R. Faeder, M.L. Blinov, and W.S. Hlavacek. Rule-based modeling of biochemical systems with BioNetGen. *Methods in Molecular Biology*, 500:113–167, 2009.

[14] N. Geva-Zatorsky, N. Rosenfeld, S. Itzkovitz, R. Milo, A. Sigal, E. Dekel, T. Yarnitzky, Y. Liron, P. Polak, G. Lahav, and U. Alon. Oscillations and variability in the p53 system. *Molecular Systems Biology*, 2:2006.0033, 2006.

[15] D. T. Gillespie. A general method for numerically simulating the stochastic time evolution of coupled chemical reactions. *Journal of Computational Physics*, 22(4):403–434, 1976.

[16] H. Gong, Y. Guo, A. Linstedt, and R. Schwartz. Discrete, continuous, and stochastic models of protein sorting in the Golgi apparatus. *Physical Review E*, 81(1):011914, 2010.

[17] H. Gong, H. Sengupta, A. Linstedt, and R. Schwartz. Simulated de novo assembly of Golgi compartments by selective cargo capture during vesicle budding and targeted vesicle fusion. *Biophysical Journal*, 95:1674–1688, 2008.

[18] H. Gong, P. Zuliani, A. Komuravelli, J. R. Faeder, and E. M. Clarke. Analysis and verification of the HMGB1 signaling pathway. *BMC Bioinformatics (to appear)*, 2010.

[19] D. Hanahan and R. A. Weinberg. The hallmarks of cancer. *Cell*, 100(1):57–70, 2000.

[20] M. Hinz, D. Krappmann, A. Eichten, A. Heder, C. Scheidereit, and M. Strauss. NF-κB function in growth control: regulation of cyclin D1 expression and G0/G1-to-S-phase transition. *Mol. Cell Biol.*, 19:2690–2698, 1999.

[21] W. S. Hlavacek, J. R. Faeder, M. L. Blinov, R. G. Posner, M. Hucka, and W. Fontana. Rules for modeling signal-transduction system. *Science STKE 2006*, re6, 2006.

[22] A. Hoffmann, A. Levchenko, M.L. Scott, and D. Baltimore. The IκB-NFκB signaling module: Temporal control and selective gene activation. *Science*, 298:1241–1245, 2002.

[23] Z. Huang. Bcl-2 family proteins as targets for anticancer drug design. *Oncogene*, 19:6627–6631, 2000.

[24] S. Idel, H.M. Dansky, and J.L. Breslow. A20, a regulator of NFκB, maps to an atherosclerosis locus and differs between parental sensitive C57BL/6J and resistant FVB/N strains. *Proceedings of the National Academy of Sciences*, 100:14235–14240, 2003.

[25] S. K. Jha, E. M. Clarke, C. J. Langmead, A. Legay, A. Platzer, and P. Zuliani. A Bayesian approach to model checking biological system. In *CMSB*, volume 5688 of *LNCS*, pages 218–234, 2009.

[26] R. Kang, D. Tang, N. E. Schapiro, K. M. Livesey, A. Farkas, P. Loughran, Bierhaus, M. T. Lotze, and H. J. Zeh. The receptor for advanced glycation end products (RAGE) sustains autophagy and limits apoptosis, promoting pancreatic tumor cell survival. *Cell Death and Differentiation*, 17(4):666–676, 2009.

[27] S. Krishna, M.H. Jensen, and K Sneppen. Minimal model of spiky oscillations in NF-kB signaling. *Proceedings of the National Academy of Sciences*, 103:10840–10845, 2006.

[28] C. J. Langmead. Generalized queries and bayesian statistical model checking in dynamic bayesian networks: Application to personalized medicine. In *CSB*, pages 201–212, 2009.

[29] S. Larris and A. J. Levine. The p53 pathway: positive and negative feedback loops. *Oncogene*, 24:2899–2908, 2005.

[30] D.F. Lee and M.C. Huang. Advances in targeting IKK and IKK-related kinases for cancer therapy. *Clinical Cancer Research*, 14:5656, 2008.

[31] T. Lipniacki, T. Hat, J. R. Faeder, and W. S. Hlavacek. Stochastic effects and bistability in T cell receptor signaling. *Journal of Theoretical Biology*, 254:110–122, 2008.

[32] T. Lipniacki, P. Paszek, A. Brasier, B. Luxon, and M. Kimmel. Crosstalk between p53 and nuclear factor-kB systems: pro-and anti-apoptotic functions of NF-kB. *Journal of Theoretical Biology*, 228:195–215, 2004.

[33] M. T. Lotze and K. Tracey. High-mobility group box 1 protein (HMGB1): nuclear weapon in the immune arsenal. *Nature Reviews Immunology*, 5:331–342, 2005.

[34] C. McInnes. Progress in the evaluation of CDK inhibitors as anti-tumor agents. *Drug Discovery Today*, 13(19-20):875–881, 2008.

[35] B. Mengel, S. Krishna, M. H. Jensen, and A. Trusina. Theoretical analyses predict A20 regulates period of NF-κB oscillation. *arXiv: bio-ph 0911.0529*, 2009.

[36] D.E. Nelson, A.E.C. Ihekwaba, et al. Oscillations in NF-κB signaling control the dynamics of gene expression. *Science*, 306:704–708, 2004.

[37] J. R. Nevins. The Rb/E2F pathway and cancer. *Human Molecular Genetics*, 10:699–703, 2001.

[38] K. Puszynski, B. Hat, and T. Lipniacki. Oscillations and bistability in the stochastic model of p53 regulation. *Journal of Theoretical Biology*, 254:452–465, 2008.

[39] A. Rizk, G. Batt, F. Fages, and S. Soliman. On a continuous degree of satisfaction of temporal logic formulae with applications to systems biology. In *CMSB*, volume 5307 of *LNCS*, pages 251–268, 2008.

[40] B. Rotblat, M. Ehrlich, R. Haklai, and Y. Kloog. The Ras inhibitor farnesylthiosalicylic acid (salirasib) disrupts the spatiotemporal localization of active Ras: a potential treatment for cancer. *Methods in Enzymology*, 439:467–489, 2008.

[41] C. Semino, G. Angelini, A. Poggi, and A. Rubartelli. NK/iDC interaction results in IL-18 secretion by DCs at the synaptic cleft followed by NK cell activation and release of the DC maturation factor HMGB1. *Blood*, 106:609–616, 2005.

[42] C. J. Sherr and F. McCormick. The Rb and p53 pathways in cancer. *Cancer Cell*, 2:103–112, 2002.

[43] X. Tang, D. Liu, S. Shishodia, N. Ozburn, C. Behrens, J.J. Lee, W.K. Hong, B.B. Aggarwal, and I.I. Wistuba. Nuclear factor-κB (NF-κB) is frequently expressed in lung cancer and preneoplastic lesions. *Cancer*, 107:2637–2646, 2006.

[44] J. Vakkila and M. T. Lotze. Inflammation and necrosis promote tumour growth. *Nature Reviews Immunology*, 4:641–648, 2004.

[45] J. R. van Beijnum, W. A. Buurman, and A. W. Griffioen. Convergence and amplification of toll-like receptor (TLR) and receptor for advanced glycation end products (RAGE) signaling pathways via high mobility group B1. *Angiogenesis*, 11:91–99, 2008.

[46] B. Vogelstein, D. Lane, and A. J. Levine. Surfing the p53 network. *Nature*, 408:307–310, 2000.

[47] K. B. Wee and B. D. Aguda. Akt versus p53 in a network of oncogenes and tumor suppressor genes regulating cell survival and death. *Biophysical Journal*, 91:857–865, 2006.

[48] H. Wu and G. Lozano. NF-κB activation of p53. a potential mechanism for suppressing cell growth in response to stress. *J. Biol. Chem*, 269:20067–20074, 1994.

[49] G. Yao, T. J. Lee, S. Mori, J. Nevins, and L. You. A bistable Rb-E2F switch underlies the restriction point. *Nature Cell Biology*, 10:476–482, 2008.

[50] H. L. S. Younes and R. G. Simmons. Statistical probabilistic model checking with a focus on time-bounded properties. *Information and Computation*, 204(9):1368–1409, 2006.

[51] P. Zuliani, A. Platzer, and E. M. Clarke. Bayesian statistical model checking with application to simulink/stateflow verification. In *HSCC*, pages 243–252, 2010.